A&A 456, 1121–1130 (2006)
DOI: 10.1051/0004-6361:20065300

Astronomy & Astrophysics

Early-type stars in the young open cluster IC 1805

II. The probably single stars HD 15570 and HD 15629, and the massive binary/triple system HD 15558⋆,⋆⋆

M. De Becker[1], G. Rauw[1,⋆⋆⋆], J. Manfroid[1,†], and P. Eenens[2]

[1] Institut d'Astrophysique et de Géophysique, Université de Liège, 17 allée du 6 Août, B5c, 4000 Sart Tilman, Belgium
e-mail: debecker@astro.ulg.ac.be
[2] Departamento de Astronomia, Universidad de Guanajuato, Apartado 144, 36000 Guanajuato, GTO, Mexico

Received 28 March 2006 / Accepted 1 June 2006

ABSTRACT

Aims. We address the issue of the multiplicity of the three brightest early-type stars of the young open cluster IC 1805, namely HD 15570, HD 15629 and HD 15558.
Methods. For the three stars, we measured the radial velocity by fitting Gaussian curves to line profiles in the optical domain. In the case of the massive binary HD 15558, we also used a spectral disentangling method to separate the spectra of the primary and of the secondary in order to derive the radial velocities of the two components. These measurements were used to compute orbital solutions for HD 15558.
Results. For HD 15570 and HD 15629, the radial velocities do not present any significant trend attributable to a binary motion on time scales of a few days, nor from one year to the next. In the case of HD 15558 we obtained an improved SB1 orbital solution with a period of about 442 days, and we report for the first time on the detection of the spectral signature of its secondary star. We derive spectral types O5.5III(f) and O7V for the primary and the secondary of HD 15558. We tentatively compute a first SB2 orbital solution although the radial velocities from the secondary star should be considered with caution. The mass ratio is rather high, i.e. about 3, and leads to very extreme minimum masses, in particular for the primary object. Minimum masses of the order of 150 ± 50 and $50 \pm 15\,M_{\odot}$ are found respectively for the primary and the secondary.
Conclusions. We propose that HD 15558 could be a triple system. This scenario could help to reconcile the very large minimum mass derived for the primary object with its spectral type. In addition, considering new and previously published results, we find that the binary frequency among O-stars in IC 1805 has a lower limit of 20%, and that previously published values (80%) are probably overestimated.

Key words. stars: early-type – stars: binaries: spectroscopic – stars: individual: HD 15570 – stars: individual: HD 15629 – stars: individual: HD 15558

1. Introduction

The study of stellar populations of young open clusters has been the purpose of many works in the last years (e.g. Sagar et al. 1988; Raboud & Mermilliod 1998). One of the crucial questions addressed in this context concerns the massive star content and the binary frequency of the earliest stars harboured by these clusters. Recent numerical simulations of the star formation in open clusters predict a high level of mass segregation, along with the formation of the most massive stars through simultaneous accretion and stellar collisions, resulting in the presence of the most massive stars in binary systems (Bonnell & Bate 2002). The investigation of the multiplicity of the massive star population of young open clusters is consequently of particular interest. For instance, García & Mermilliod (2001) presented radial velocity measurements for 37 O- and B-stars in the open cluster NGC 6231, and proposed binary frequencies for a series of open clusters, among which is IC 1805.

IC 1805 is a young rich open cluster in the core of the Cas OB6 association, in the molecular cloud W 4 in the Perseus spiral arm of our Galaxy. Massey et al. (1995) inferred an age of 1–3 Myr for the cluster, in agreement with other previous estimates (see Feinstein et al. 1986, and references therein, although these latter authors proposed an age < 1 Myr). The spectroscopic study of Shi & Hu (1999) revealed that about 80 of the members of IC 1805 are O or B stars. García & Mermilliod (2001) (see also Ishida 1970) estimated a binary frequency of 80% among the 10 O-stars in IC 1805. However, in a previous paper (Rauw & De Becker 2004, Paper I), we showed that two suspected binaries, BD +60° 501 (O7V((f))) and BD +60° 513 (O7.5V((f))), were most probably single stars, suggesting that the binary frequency proposed by García & Mermilliod (2001) might be overestimated. In this paper, we investigate the multiplicity of the three earliest O-type stars of the cluster: HD 15570, HD 15629, and HD 15558.

HD 15570 (O4If^{+}, $V = 8.10$) was proposed to be the most massive member of IC 1805, and incidentally one of the most massive and most luminous stars known in our Galaxy, with a present evolutionary mass of about $80\,M_{\odot}$ following

⋆ Based on observations collected at the Observatoire de Haute-Provence (France).
⋆⋆ Appendices are only available in electronic form at http://www.edpsciences.org
⋆⋆⋆ Research Associate FNRS (Belgium).
† Research Director FNRS (Belgium).

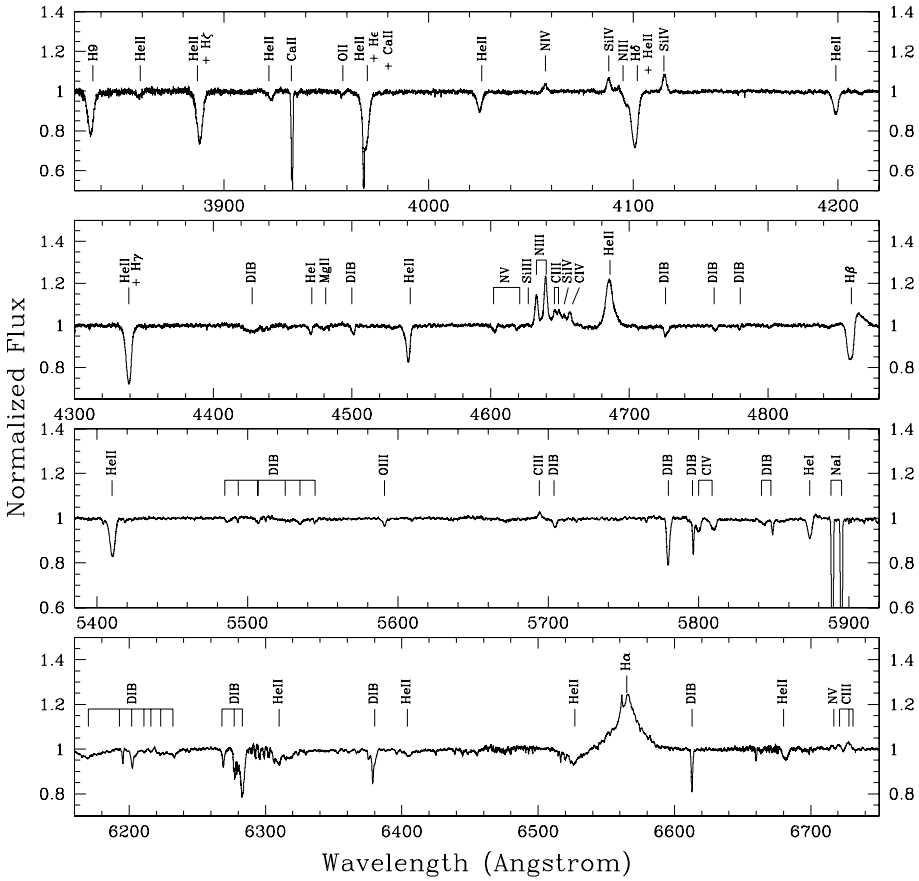

Fig. 1. Mean spectrum of HD 15570 calculated from spectra obtained at SPM between HJD 2 453 287.93 and HJD 2 453 290.00.

Herrero et al. (2000). HD 15629 (O5V((f)), $V = 8.42$) has also been proposed to be a very massive star. According to Herrero et al. (2000), this star could have evolved from an initial mass of about 70 $M_\odot$, and presently be on the way towards evolutionary stages close to those of HD 14947 (O5If$^+$) and HD 210839 (O6I(n)fp, λ Cep). The same authors inferred a present-day evolutionary mass of about 61 $M_\odot$. For both stars, no clear evidence of binarity has been reported in the literature, even though some radial velocities quoted in the WEBDA data base[1] suggest the occurrence of variations.

HD 15558 ($m_V = 8.0$) was classified as an O5III(f) star by Mathys (1989). It was reported to be a spectroscopic binary with a period of about 420 d for the first time by Trumpler (according to Underhill 1967). Up to now, the only orbital solution proposed for this system is that of Garmany & Massey (1981), revealing a highly eccentric binary ($e = 0.54$) with a period of about 440 d, i.e. the longest of any O-type spectroscopic binary known at that time. This star is also believed to be very massive. Herrero et al. (2000) derived spectroscopic and evolutionary masses of about 90 $M_\odot$ for HD 15558. Finally, this massive binary is classified as a non-thermal radio emitter. In this context, the study of its binarity is of crucial interest (see De Becker 2005, for a detailed discussion).

This paper is organized as follows. Section 2 presents the optical spectrum of the stars. The results of the radial velocity study for HD 15570 and HD 15629 are given in Sect. 3. The case of HD 15558 is discussed in detail in Sect. 4. Section 5 consists of a discussion of our results. A summary of the main results and the conclusions are provided in Sect. 6.

[1] Available at `http://obswww.unige.ch/webda`.

2. The optical spectrum

2.1. HD 15570

A detailed description of our data is given in Appendix A. The most prominent features observed in the spectrum presented in Fig. 1 are the He II λ 4686 and Hα lines, in strong emission. The He II λ 4686 emission is one of the characteristics of the Of$^+$ type, along with Si IV $\lambda\lambda$ 4088–4115 also in emission and N III $\lambda\lambda$ 4634–4641. We find also weaker emission lines of N IV at 4058 Å, C III at 4650 and 5696 Å, and also C IV λ 4662. The weak emission lines at 6721, 6728 and 6731 Å might be attributed to C III (Walborn 2001). We report also on the probable presence of Si IV λ 4656 and N V $\lambda\lambda$ 6716,6718 in emission (Walborn 2001). The Hβ line appears as a P Cygni profile with a very deep absorption component. Other absorption lines are mainly due to He II. He I λ 4471 is very weak. We also note that the He I λ 5875 line appears as a P Cygni profile, even though the emission component is rather weak. The Mg II λ 4481 line is detected, and we also note the presence of the N V $\lambda\lambda$ 4604,4620 lines in absorption. Even though its presence is not obvious in the mean SPM spectrum (see Fig. 1), a weak emission feature at about 4487 Å is observed in OHP spectra and is probably due to S IV (Werner & Rauch 2001).

Using the classification criterion given by Mathys (1988), we infer the spectral type O4. The various emission lines discussed above lead to the O4If$^+$ spectral type for HD 15570, in agreement with Walborn's classification (Walborn 1972). A comparison with the spectrum of the O4If$^+$ star HD 269698 (Walborn & Fitzpatrick 1990) lends further support to this classification.

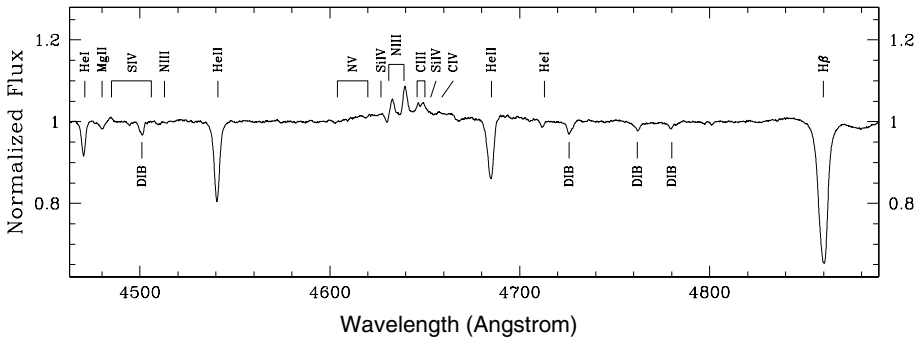

Fig. 2. Mean normalized spectrum of HD 15629 between 4465 Å and 4890 Å as observed in September 2002 at OHP.

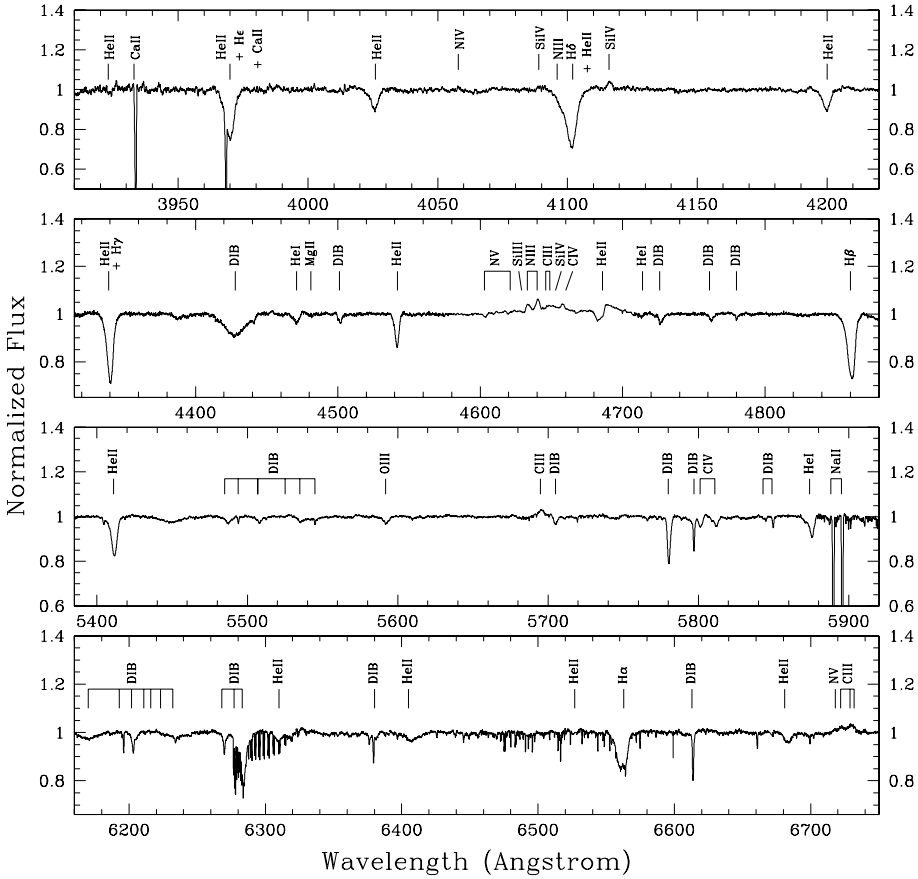

Fig. 3. Spectrum of HD 15558 obtained about at phase 0.8, i.e. at the maximum of the radial velocity curve presented in Fig. 4. This spectrum was obtained with the Elodie echelle spectrograph on 7 January 2004, except for the spectral domain between 4580 and 4710 Å which is taken from one of the spectra obtained in September 2001 with the Aurélie spectrograph. We note that a large portion of the spectrum was skipped because of a lack of important spectral features.

2.2. HD 15629

The strongest lines in the blue spectrum of HD 15629 (Fig. 2) are in order of decreasing intensity: Hβ, He II λ 4542, He II λ 4686 and He I λ 4471, all in absorption. The He I λ 4713 absorption line is very weak. The Mg II λ 4481 absorption line is also present. The N III $\lambda\lambda$ 4634–4641 lines are the strongest emission features observed in this spectrum. The C III blend at about 4650 is also present and we note the possible presence of C IV λ 4662 in weak emission. The weak emission feature at about 4487 Å is probably due to S IV (Werner & Rauch 2001).

Adopting the classification criterion porposed by Mathys (1988), we derive an O5 spectral type. Considering that the N III $\lambda\lambda$ 4634-4641 features are in emission, and that He II λ 4686 is in strong absorption, we adopt the O5V((f)) spectral type for HD 15629, in agreement with previous classifications.

2.3. HD 15558

In Fig. 3, we present the spectrum of HD 15558 between 3910 and 6750 Å obtained with the Elodie spectrograph on 7 January 2004, i.e. close to the maximum of the radial velocity curve presented in Fig. 4. We note that the orders of the echelle spectra obtained with Elodie are rather narrow, rendering the rectification procedure somewhat difficult where the wings of several lines merge over several tens of Å. So, for the purpose of the presentation of the optical spectrum of HD 15558, the spectral

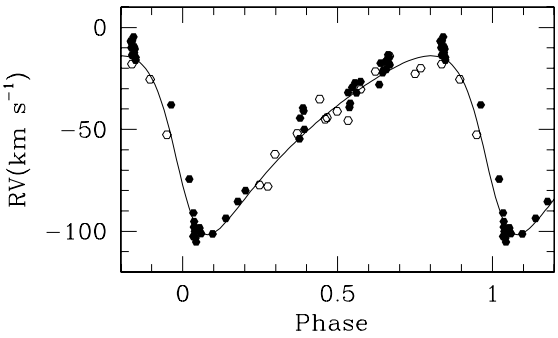

Fig. 4. Radial velocity curve of HD 15558 for an orbital period of 442 d. The open and filled hexagons stand respectively for the primary RVs obtained with Elodie and Aurélie spectra. The solid line yields our best fit orbital solution respectively corresponding to the parameters provided by Table 1. The mean of the RVs of the He II λ 4542 and of the N III $\lambda\lambda$ 4634, 4641 lines was used to compute this orbital solution.

domain between 4580 and 4710 Å in Fig. 3 comes from one of the Aurélie spectra obtained during the September 2001 observing run, i.e. very close to the orbital phase of the selected Elodie spectrum.

The strongest absorption features are the hydrogen Balmer lines. The He II lines appear also in absorption, except for He II λ 4686 which displays a P-Cygni profile. The He I absorption lines at 4471 and 5875 Å are also present, along with He I λ 4713 which is very weak. The other absorption features observed in the spectrum are Mg II λ 4481, N V $\lambda\lambda$ 4604, 4620, Si III λ 4627, O III λ 5592 and C IV $\lambda\lambda$ 5801,5812. The strongest emission lines are the N III $\lambda\lambda$ 4634,4641 lines. We report also on noticeable C III lines at 4650, 4652, 5696, 6721, 6728 and 6731 Å. The three latter lines were qualified as selective emission lines by Walborn (2001) as well as the N V $\lambda\lambda$ 6716, 6718 emission features. We report also on the presence of the Si IV λ 4116 emission line, along with that of the much weaker Si IV λ 4088. Finally, the C IV λ 4662 emission line is cleary present. The spectral classification of the stars in this binary system is detailed in Sect. 5.1.

3. The probably single stars HD 15570 and HD 15629

Both stars have been mainly observed at the Observatoire de Haute-Provence (OHP, France) with the 1.52 m telescope. Some spectra were also obtained with the 2.1 m telescope at the Observatorio Astronómico Nacional of San Pedro Martir (SPM, Mexico). For details on the observations and the data reduction procedure, see Appendix A. We have measured the radial velocity (RV) of the strongest lines for HD 15570 and HD 15629 by fitting Gaussians to the line profiles. The RVs of various lines from OHP data only are quoted in Table B.1.

In the case of HD 15570, the dispersion of the RV of the He I λ 4471 line is larger than for other lines in most of our data sets, as its profile deviates significantly from a Gaussian. In the case of the He II λ 4542 line, we performed a Fourier analysis of the RVs following the method described by Heck et al. (1985) and revised by Gosset et al. (2001). The periodogram reveals several peaks. The highest one is found at a frequency of 0.71 d^{-1}. However, the corresponding semi-amplitude is very low (about 4 km s^{-1}) compared to the typical error on the RVs. This error, i.e. about 10 km s^{-1}, corresponds to the standard deviation determined for the radial velocity of a Diffuse Interstellar Band (DIB) at about 4762 Å. The radial velocities of the N III emission lines appear stable on the time scales investigated in this study. As a result, we do not detect any significant RV variation attributable to binarity on time scales of a few days, nor from one year to the next, in our OHP data. The radial velocities measured on the main absorption and emission lines observed in the SPM spectra did not reveal any significant RV change neither on a time scale of a few days, although we may note that the dispersion obtained in most cases is larger due to non-Gaussian profiles and to a poorer quality of the data. The lack of significant RV variations is not in agreement with the RV changes suggested by the data collected in the WEBDA data base. We caution however that these archive RV measurements were obtained on the basis of sometimes heterogeneous line lists and with instruments of different capabilities, at very different epochs.

The strong profile variability displayed by the He II λ 4686 and Hβ lines (see De Becker 2005), along with their noticeable asymmetry, prevented us from obtaining accurate and reliable RVs from the entire profiles of these lines. Still, we mention that the RVs measured at the top (resp. bottom) of the He II λ 4686 (resp. Hβ) line reveal rather strong wavelength shifts, which are correlated both in direction and amplitude (semi-amplitude of $\sim$30 km s^{-1}) for the two lines. However, the lack of significant shift for the RVs of He I λ 4471, He II λ 4542 and N III $\lambda\lambda$ 4634-4641 does not support the idea that this could be due to the orbital motion in a binary system. We finally note that the RVs of the Balmer lines measured on SPM spectra display the expected progression due to the transition from purely absorption (H9) to P-Cygni (Hβ) profiles.

For HD 15629, we measured the RV for several lines that are free from profile variability. Therefore, only the He I λ 4471, He II λ 4542, and N III $\lambda\lambda$ 4634–4641 lines are considered in this discussion. A Fourier analysis of the RVs from the three data sets reveals a highest peak at 0.08 d^{-1} (P = 12.6 d) for He I λ 4471, and at 0.16 d^{-1} (P = 6.25 d) for He II λ 4542. The periodogram for this latter line presents also a peak close to that of the He I line at 0.09 d^{-1} (P = 11.1 d). However, the amplitude of these peaks is only about 5 km s^{-1}. We detect no significant RV variations for any of the lines. This result is in contrast with the variable status reported by Underhill (1967) and Humphreys (1978). We also mention that long term RV variations were reported for this star (see the WEBDA data base), but we should consider these values with caution for the same reasons as for HD 15570 (see above). In summary, we did not find any trend pointing to a binary scenario on the time scales sampled by our data.

4. The massive binary HD 15558

4.1. Radial velocity time series

As mentioned in Sect. 1, the only orbital solution available for HD 15558 was proposed by Garmany & Massey (1981). These authors reported on a period of 439.3 ± 1.0 d, with an eccentricity of 0.54 ± 0.05. However, their orbital solution was based on time series including a somewhat heterogeneous set of radial velocities. They indeed used mean RVs calculated on the basis of 4 to 12 different lines. Among these lines, many are expected to be at least partly produced in the stellar wind, and might therefore not reflect the RV of the star itself. The heterogeneity of their RV time series could have a significant impact on the orbital parameters. In this section, we describe the procedure we adopted to establish our RV time series, and how we use it to determine the SB1 orbital parameters of the system.

The details on our data on HD 15558 are given in Appendix A. First of all, we focused on the wavelength range covered by all our spectra, whatever the instrumentation used, i.e. the spectral domain between 4455 and 4680 Å. We then selected the lines whose profile did not deviate too strongly from a typical Gaussian shape. Only the He II λ 4542 and the N III $\lambda\lambda$ 4634, 4641 lines meet our criteria. We then determined the RVs by fitting Gaussians to the profiles. In the case of Elodie data, the He II line is simultaneously observed in two adjacent orders. We therefore measured the RV on each order and we used the mean of the two values in our time series. The RVs obtained from these three lines, along with those obtained from other lines observed only in our echelle spectra, are compiled in Table B.2. In this Table, the column labeled "Mean" contains the mean RVs obtained from the three lines discussed above. We estimate that the expected uncertainty on the RVs are respectively of the order of 15–20, 10–15, and 5–8 km s^{-1} respectively for low resolution Aurélie, medium resolution Aurélie, and high resolution Elodie data. However, we mention that the error on the RVs measured on some low quality Elodie spectra may be significantly larger. These uncertainties were estimated on the basis of radial velocity measurements performed on DIBs.

4.2. Period determination

We performed a Fourier analysis on our RV time series following the technique described by Heck et al. (1985) and revised by Gosset et al. (2001), as used for instance in Paper I and by De Becker et al. (2004) for other spectroscopic binaries. We independently applied the same technique to three RV time series obtained respectively from He II λ 4542, a mean of the RVs from the two N III $\lambda\lambda$ 4634, 4641 lines, and a mean of the He II and N III lines. In the three cases, the periodogram is dominated by a strong peak at a frequency of 0.00226 d^{-1}, corresponding to a period of about 442 d. As the time base covered by our data is about 1608 d, the typical width of the peaks of the periodograms is about 6.22×10^{-4} d^{-1}. Considering that the uncertainty on the frequency is about 10% of the width of the peak, we obtain an uncertainty on the period of about 12 d. The fact that the three RV time series lead exactly to the same period is a strong argument for this value being the true period of the system.

4.3. Orbital solution

We obtained the SB1 orbital solution of HD 15558 using the method of Wolfe et al. (1967) for SB1 systems. We assigned different weights to take into account the expected uncertainties affecting our RV measurements. These weights vary between 0.1 and 1.0 respectively for very poor quality and good quality Elodie data. Aurélie RVs get intermediate weights to take into account the fact that though the resolution of the spectrograph is rather low, the quality of the data is much better than for Elodie spectra.

We first fixed the period to the value determined from the Fourier analysis of our RV time series, i.e. ~ 442 d. We obtained similar results for the orbital parameters, i.e. for most of them within the error bars, whatever the RV time series used. We also calculated the orbital solution through an iterative process allowing the period to vary, but it did not improve significantly the results. We indeed obtained a period of about 445 d, which can not be distinguished from the 442 d period obtained in Sect. 4.2 provided the uncertainty on the period is about 12 d. Therefore, we adopted the results obtained with a period fixed to 442 d. The corresponding orbital parameters are quoted in Table 1 for the series of RVs obtained respectively on the basis of the He II and N III lines (*left column*), and on the basis of the He II line only (*right column*).

Table 1. Orbital parameters of the SB1 solution of HD 15558. $T_\circ$ refers to the time of periastron passage. γ, K, and $a \sin i$ denote respectively the systemic velocity, the amplitude of the radial velocity curve, and the projected separation between the centre of the star and the centre of mass of the binary system. The last row provides the mass function. The orbital elements are given for the solutions obtained respectively from the mean of the RVs of the He II λ 4542 and N III $\lambda\lambda$ 4634, 4641 lines, and from the RVs of He II λ 4542 only. $T_\circ$ is expressed in HJD–2 450 000.

	He II λ 4542 N III $\lambda\lambda$ 4634, 4641	He II λ 4542
P (days)	442 (fixed)	
e	0.39 ± 0.03	0.40 ± 0.03
$T_\circ$	1795.400 ± 6.556	1798.385 ± 7.207
γ (km s^{-1})	–50.2 ± 1.1	–40.1 ± 1.1
K (km s^{-1})	43.9 ± 1.8	41.3 ± 1.8
ω	116° ± 6°	121° ± 7°
$a \sin i$ ($R_\odot$)	350.0 ± 15.2	331.2 ± 15.2
$f(m)$ ($M_\odot$)	3.0 ± 0.4	2.5 ± 0.3

4.4. Searching for the companion

We inspected more carefully spectra obtained at phases close to the extrema of the radial velocity curve presented in Fig. 4. Though we did not obtain any echelle spectra close to the minimum of the primary radial velocity curve, the September 2000 and September 2001 Aurélie observing runs fall respectively very close to the minimum and maximum of the radial velocity curve. We were therefore able to perform a more careful inspection of the line profiles on the basis of our Aurélie spectra. We added together the 12 spectra obtained during each observing run to obtain two high signal-to-noise ratio spectra, respectively of about 1000 at the minimum and 900 at the maximum. We detected opposite asymmetries at both extrema for the profiles of the He I λ 4471, Mg II λ 4481 and He II λ 4542 lines, suggesting clearly the presence of the secondary. The inspection of the Elodie spectrum closest to the maximum of the primary RV curve reveals also the signature of the secondary in the profile of the C IV λ 5812 and He I λ 5876 lines.

The upper and lower panels of Fig. 5 show the profile of the He I λ 4471, Mg II λ 4481 and He II λ 4542 lines respectively at the minimum and at the maximum of the primary radial velocity curve. We disentangled the profiles from the primary and the secondary by fitting Gaussians following an iterative process. We constructed fitting functions of the form given by Eq. (1):

$$P(\lambda) = \sum_{j}^{N} \frac{A_j}{\sigma_j \sqrt{2\pi}} \exp\Big[- \frac{(\lambda - \lambda_{c,j})^2}{2\sigma_j^2}) \Big] \quad (1)$$

with $N = 2, 3, 4$ following the complexity of the blended profile. The three parameters to be determined for each Gaussian are respectively the normalization factor (A_j), the standard deviation of the Gaussian (σ_j), and the central position ($\lambda_{c,j}$). We iteratively changed the values for the three parameters with $N = 2$ to obtain a first order fit of the primary and of the secondary for the helium lines. We then increased the number of Gaussian components in our fit to account for the presence of the N III λ 4537 line

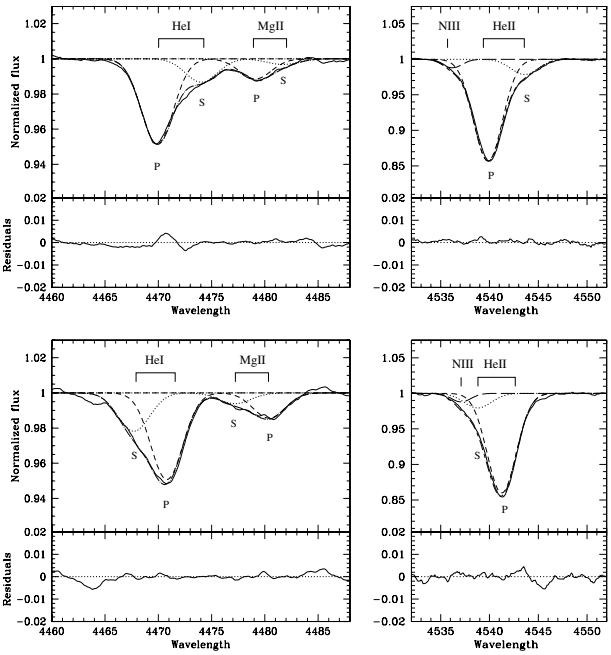

Fig. 5. Disentangling of the line profiles from the two components of HD 15558 respectively at the minimum of the radial velocity curve (*upper part of the figure*), and at the maximum of the radial velocity curve (*lower part of the figure*). The two data sets correspond to the mean spectra obtained respectively during the September 2000 and September 2001 observing runs with the 1.52 m OHP telescope. The profiles of the He I λ 4471, the Mg II λ 4481, and the He II λ 4542 lines are displayed, along with the best-fit functions (dotted-dashed lines). The individual Gaussians are also displayed, with the dashed and dotted lines standing respectively for the primary (P) and the secondary (S). The bottom part of each panel represents the residuals (in the sense data – fit).

on the blue side of the He II λ 4542 line. We optimized the fit of the He II line by fitting the N III line in the blend at the minimum of the radial velocity curve of the primary, i.e. when the secondary He II line is shifted to the red and consequently well separated from the N III line. We then fixed the width and the normalization factor of the N III line to the same values to fit the helium components of the blended profile at the maximum of the RV curve. We used a $N = 4$ function to fit the blend of the He I λ 4471 line with that of Mg II at 4481 Å (primary and secondary). The synthetic profiles obtained on the basis of Eq. (1) are overplotted on the observed profiles in Fig. 5. While performing these fits, we first fixed the width and the normalization coefficient of the primary component to the same values at both extrema. We then improved the fits by allowing these parameters to vary.

On the basis of our best fits, we estimated the equivalenth width (*EW*) of the He I and He II lines to obtain a spectral classification of the two components of the system. At the maximum of the RV curve, we obtain *EW*s of 0.18 ± 0.02 and 0.53 ± 0.03 Å respectively for the He I λ 4471 and He II λ 4542 lines of the primary. At the same phase but for the secondary, we obtain respectively *EW*s of 0.05 ± 0.02 and 0.08 ± 0.02 Å. Using the classification criteria proposed by Mathys (1988), we obtain O5 and O6.5 spectral types respectively for the primary and the secondary. The best-fit parameters obtained at the phase corresponding to the minimum of the SB1 RV curve lead to *EW*s of 0.19 ± 0.02 and 0.52 ± 0.03 Å (respectively 0.08 ± 0.02 and 0.07 ± 0.03 Å) for the He I and He II lines of the primary (resp. secondary). In this case, the spectral types of the two components of HD 15558 are O5.5 and O7.5. Considering mean values of the *EW*s obtained at the extreme phases of the orbit, the classification of the two components of the system are O5.5 and O7 respectively for the primary and the secondary.

We note that the *EW* of He I λ 4471 undergoes a significant decrease (~40%) as the secondary is receding from the observer. Such a decrease is also marginally observed for the Mg II line, but no such behaviour is detected for the He II λ 4542 line. However, the *EW*s of the primary remain steady from one extremum to the other. This behaviour is quite reminiscent of the so-called Struve-Sahade effect observed in the case of several massive binary system (see e.g. Bagnuolo et al. 1999). However, we note that, for such weak lines as in HD 15558, it might be due to errors in the normalization of the spectra.

4.5. Estimation of the masses of the components of HD 15558

As we were able to separate the primary and secondary components from the profiles of a few lines at both extrema of the RV curve, we obtained a first estimate of the amplitude of the secondary RV curve. In the case of the He II λ 4542 line, we estimated that the RV of the secondary was determined with an uncertainty of about $15\,\mathrm{km\,s^{-1}}$ at its maximum, and about $20\,\mathrm{km\,s^{-1}}$ at its minimum. This difference is due to the fact that the blend with the N III line makes the determination of the parameters of the secondary component of the He II line more difficult (see bottom right panel of Fig. 5). According to our fit, and using the K value derived from our SB1 fit (see Table 1), we obtain a mass ratio of 3.3 ± 0.4. The explicit expression of the mass function as a function of the period (P), the eccentricity (e), the primary RV semi-amplitude (K) and the mass ratio (q) allowed us to estimate the minimum masses of the two components. We obtain minimum masses of 152 ± 51 and $46 \pm 11\,M_\odot$ respectively for the primary and the secondary. We note that the large errors on the minimum masses are clearly dominated by the large uncertainty on the mass ratio.

The very large masses of the two stars, mainly of the primary, are compatible with the large values already mentioned in the literature for this star (see e.g. Herrero et al. 2000). This is the first time that spectroscopic data lend support to this assertion. However, we emphasize that the minimum masses are poorly constrained. The critical issue regarding our results is the estimate of the mass ratio. More RV measurements are needed close to the extrema of the radial velocity curve to reduce the uncertainty on q, and accordingly reduce the error bars on the minimum masses. In order to address this issue and to tentatively derive the first SB2 orbital solution for this system, we applied a distentangling method to our spectral time series.

4.6. Disentangling of the primary and secondary spectra of HD 15558

We used the spectral disentangling method described by González & Levato (2006). It consists of an iterative procedure allowing to compute the spectra and RVs of the two components of a binary system. At the starting point, a flat spectrum is adopted for the secondary, and the phase-shifted mean of the observed spectra is used as the starting primary spectrum. At each iteration, the spectra of the primary and the secondary obtained at the previous step are subtracted from the observed spectra, and the radial velocities are determined on the residuals through

Table 2. Orbital parameters of the SB2 solution of HD 15558 determined from the RVs computed with the disentangling procedure of González & Levato (2006). We started the iteration procedure with the mean of the He II λ 4542 and the N III $\lambda\lambda$ 4634–4641 lines (*left part*) and of the He II λ 4542 line alone (*right part*). The parameters have the same meaning as in Table 1. R_{RL} stands for the radius of a sphere with a volume equal to that of the Roche lobe computed according to the formula of Eggleton (1983).

	He II & N III		He II	
	Primary	Secondary	Primary	Secondary
P (days)	~442 (fixed)			
e	0.41 ± 0.06		0.37 ± 0.07	
$T_\circ$ (HJD–2 450 000)	1790.377 ± 11.935		1796.271 ± 12.970	
ω	100° ± 10°		120° ± 12°	
γ (km s^{-1})	–54.1 ± 8.2	0.6 ± 11.4	–51.5 ± 12.3	–10.2 ± 15.3
K (km s^{-1})	48.3 ± 4.6	157.9 ± 15.2	43.3 ± 6.3	135.9 ± 19.7
$a \sin i$ ($R_\odot$)	385.6 ± 38.8	1259.5 ± 126.6	351.4 ± 52.0	1101.3 ± 163.0
$m \sin^3 i$ ($M_\odot$)	234.0 ± 61.4	71.6 ± 15.8	159.5 ± 58.4	50.9 ± 14.4
$q = m_1/m_2$	3.27 ± 0.45		3.13 ± 0.71	
$R_{RL} \sin i$ ($R_\odot$)	186.5 ± 19.3	355.8 ± 37.9	168.6 ± 26.0	314.6 ± 52.3

a cross-correlation procedure using a template including a series of lines. The advantage of this procedure is the fact that it does not require any accurate a priori knowledge of the spectrum of the two stars.

As our spectral time series include data obtained with different instrumentations, we once again limited our investigation to a wavelength domain covered by all our data. We applied the disentangling procedure to our 70 spectra between 4456 and 4567 Å, in order to include the He I λ 4471, the Mg II λ 4482 and the He II λ 4542 lines. These lines were selected because they display rather clearly the signature of both components of the system. Starting from the two sets of RVs used to obtain the SB1 solutions described in Table 1, we applied this technique in three different situations:

(a) First, we used all our spectra and we allowed both primary and secondary RVs to vary. The RVs obtained after 20 iterations were used to compute an SB2 orbital solution, following the technique described by Sana et al. (2003). The orbital parameters are given in Table 2. The most striking results are the huge minimum masses for the stars, mostly for the primary, in agreement with the values discussed in Sect. 4.5. We see that most parameters have values close to those obtained for the SB1 orbital solution (see Table 1). Even the difference in the semi-amplitude of the primary radial velocity curve is rather small, whilst the RVs were estimated on the basis of two very different approaches. The Gaussian fit used for the SB1 case likely underestimates the amplitude of the RV curve, but Fig. 5 suggests that the shift between the blended profile and the primary component centroids should be very small. In the case of the mean He II and N III (resp. He II alone) RVs, we note that the disentangling of four (resp. one) spectra gave unsatisfactory results as the derived RVs deviated strongly from those of other spectra obtained only a few days before or after. The disentangling program yields indeed unreasonable radial velocities for the secondary, mostly in the case of spectra with poor signal-to-noise ratios (all deviant points come from Elodie data). For this reason, we discarded these spectra from the computation of the orbital solutions presented in Table 2. In Fig. 6, we present the radial velocity curves obtained for both components of the system. We see that the agreement between the data and the computed RV curve for the secondary is rather poor, mostly at phases where the separation between the two components is small. The separated spectra of the primary and of the secondary in the wavelength domain used for the disentangling procedure are individually displayed in Fig. 7.

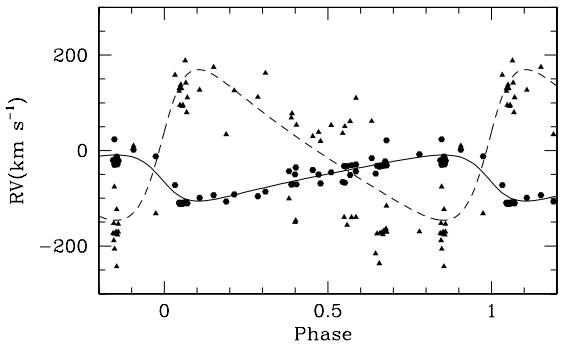

Fig. 6. Radial velocity curves of the two components of HD 15558 for an orbital period of ~442 d. The hexagons (resp. triangles) stand for the primary (resp. secondary) RVs. The solid and dashed line yield our best fit orbital solution respectively for the primary and the secondary, with the parameters provided in the left part of Table 2.

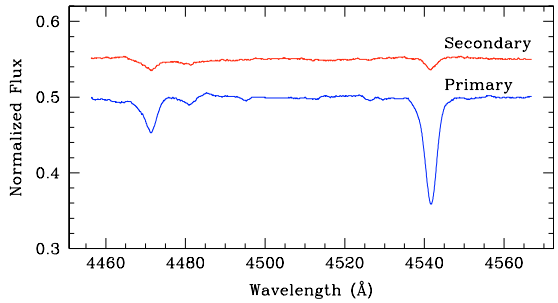

Fig. 7. Separated spectra of the primary (*lower spectrum*) and of the secondary (*upper spectrum*) of HD 15558 in the wavelength domain used for the disentangling procedure.

(b) We then applied the same procedure, but we fixed the radial velocities of the primary to the values taken for the SB1 solution. We obtained rather similar results as in case (a) although the RVs derived for the secondary in the case of several spectra were not acceptable.

(c) We finally applied the spectral disentangling method to a reduced spectral series, including only 32 spectra obtained at phases close to the extrema of the radial velocity curve, i.e.

between phases 0.05 and 0.25 and between phases 0.75 and 0.95. We selected these spectra in order to obtain an estimate of the mass ratio unaffected by the data obtained when the primary and secondary components are heavily blended. This approach leads to a mass ratio of 3.7 ± 1.2, but we note that this value should be considered with caution as the eccentricity (0.1 ± 0.1) and the T_o deviate significantly from the values derived from the SB1 and the SB2 (cases a and b) solutions.

In summary, we find that the mass ratio of the two components of the system obtained from radial velocities determined on the basis of the disentangling method is of the order of 3, whatever the initial RVs considered as the starting point of the procedure. This value is in agreement with the mass ratio derived from the simultaneous fit of Gaussians discussed in Sect. 4.5, but we failed to reduce the uncertainty on q. Consequently, the minimum masses estimated with both approaches are similar. The extreme minimum masses seem therefore to be robust. For initial RVs obtained with the He II λ 4542 line, both methods provide minimum masses of the order of 150 ± 50 and $50 \pm 15\,M_\odot$ respectively for the primary and the secondary. For RVs obtained from the He II and N III lines, the minimum masses are somewhat larger with a larger uncertainty. Although the uncertainty on the secondary radial velocities is large, the fact that our results rely partly on several spectra obtained close to the extrema of the radial velocity curves lends some support to the mass ratios derived by our analysis.

5. Discussion

5.1. Detailed spectral classification of HD 15558

As shown by De Becker (2005), the He II λ 4686 line shows a P-Cygni profile for the primary and is in absorption for the secondary. These profiles, along with the luminosity contrast between the primary and the secondary, are compatible with a difference of one luminosity class between the two stars. Considering the fact that Hα is in absorption (see Fig. 2), it is unlikely that the primary is a supergiant and we therefore propose giant and main-sequence luminosity classes respectively for the primary and the secondary. On the other hand, it is not clear whether the N III $\lambda\lambda$ 4634, 4641 lines are in emission for the secondary as well. Consequently, we propose that the massive binary HD 15558 is formed of an O5.5III(f) primary with an O7V secondary.

5.2. A very massive primary?

The most interesting – and also puzzling – result presented in Sect. 4 is the very high minimum mass derived for the primary of HD 15558, especially considering its spectral type. On the one hand, the most massive star whose mass was determined using spectroscopic and photometric data is the massive binary WR20a, with masses of 82 and 83 $M_\odot$ respectively for the primary and the secondary (Rauw et al. 2004; Bonanos et al. 2004). On the other hand, very high stellar masses were proposed (i) for the Pistol Star, close to the Galactic center, with a mass around 200–250 $M_\odot$ (Figer et al. 1998), and (ii) for the most massive stars in the Large Magellanic Cloud with masses of the order of 120–200 $M_\odot$ (Massey & Hunter 1998).

The fact that we derive such a high mass for the primary raises the question of the so-called stellar "upper mass limit". Massive stars are expected to be vibrationally unstable above a given critical mass which depends on the evolutionary state. For zero-age main sequence stars, the most accurate calculations resulted in critical masses between about 90 and 440 solar masses (see Appenzeller 1987 for a review). Oey & Clarke (2005) statistically demonstrated that the local census of massive stars oberved so far (Milky Way + Magellanic Clouds) exhibits a "universal" upper mass cutoff around 120–200 $M_\odot$ for a Salpeter initial mass function (IMF). Considering that the largest stellar mass observed in IC 1805 is about 100 $M_\odot$, the same authors estimate that the probability that the stellar population of IC 1805 extends to 150 $M_\odot$ (resp. 200 $M_\odot$) is about 0.63 (resp. 0.51). As a consequence, a stellar mass of $150 \pm 50\,M_\odot$, assuming the minimum masses derived above are close to the true masses ($i \sim 90°$), does not disagree with both the theoretical and the statistical approaches of the stellar upper mass limit.

Provided the mass derived for the primary is indeed of the order of 150 $M_\odot$[2], the main issue comes from its spectral type. We may indeed expect the most massive stars to be also the earliest ones. Considering for instance the typical masses given by Howarth & Prinja (1989), we see that the expected masses for O5.5 stars should lie between 50 and 80 $M_\odot$ depending on the luminosity class. An O5.5III star with a mass of about 150 $M_\odot$ – i.e. about a factor 2 too high – constitutes therefore a severe anomaly with respect to the usual classification adopted for O-type stars[3]. In addition, a very massive star is also expected to be very luminous. From the observed V magnitude of HD 15558 and considering a reddening law with $R_V = 3.1$ and a color excess $E(B-V) = 0.71$[4], we derive an extinction A_V equal to 2.20, leading to an apparent dereddened V magnitude equal to 5.70. Using the relation given by Howarth & Prinja (1989), we obtain a bolometric correction of –3.86, yielding a dereddened apparent bolometric magnitude equal to 1.84. Considering a distance to IC 1805 of 2.3 kpc (Massey et al. 1995), we derive a $\log(L_{bol}/L_\odot)$ equal to about 5.9. If we consider that the primary contributes about 5/6 of the total bolometric luminosity, $\log(L_{bol}/L_\odot)$ reduces to about 5.82. This value is much too low to be compatible with a 150 $M_\odot$ primary. Indeed, a confrontation of the bolometric luminosity to theoretical evolutionary tracks for various metallicities (Schaller et al. 1992; Schaerer et al. 1993) suggests masses not higher than about 70 $M_\odot$. If the distance we assumed here is correct, such a massive primary should be much more luminous than observed.

On the other hand, an initially extremely massive and very hot early-type (i.e. spectral type O2) main sequence star will cool down during its evolution towards the giant luminosity class. For instance, according to the evolutionary models of Schaller et al. (1992), a star of initial mass 120 $M_\odot$ starts its evolution with an effective temperature of 53 000 K. When the effective temperature reaches 38 000 K, typical for an O5.5 giant (Martins et al. 2005), the stellar mass has decreased to about 85 $M_\odot$. Moreover, at this evolutionary stage, the hydrogen surface

[2] We rely on the fact that the confidence interval derived by our analysis shows that there is a 65% probability that the minimum mass of the primary lies between about 100 and 200 $M_\odot$. This does not rule completely out a situation where this mass is lower than 100 $M_\odot$.

[3] We note also that a mass of 50 $M_\odot$ for the O7V secondary is somewhat excessive. However, considering the error bar on the mass of the secondary, the 1-σ confidence interval is still compatible with the typical values proposed by Howarth & Prinja (1989) for an O7V star, i.e. 36 $M_\odot$. Consequently, we consider that the mass of the primary is the main issue worth addressing here.

[4] We obtained the color excess $E(B-V)$ using the observed $(B-V) = 0.5$ given by Massey et al. (1995) and the intrinsic color $(B-V)_0$ based on the spectral type.

abundance should already be reduced, whilst helium should be enhanced. The main conclusion here is that a very massive star would have to lose a substantial fraction of its initial mass before reaching the effective temperature of an O5.5 giant. This would then imply an extremely large initial mass for the primary of HD 15558.

Let us consider an alternative scenario, where HD 15558 is not a binary but a hierarchical triple system. The primary may be constituted of a yet unrevealed close binary system. In this scenario, as the mass of the primary is estimated on the basis of the motion of the secondary, the primary object – i.e. the hypothetical close binary – would appear to be a massive object whose mass is the sum of the masses of two stars. Provided the spectral type derived from our spectra for the primary is typical of the two stars constituting the close binary, we are possibly observing the composite spectrum of two similar O-stars, in addition to that of the secondary object whose spectral type should be O7. This scenario offers the possibility to explain the unexpected high mass of the primary object, and to reconcile its mass with its spectral type. However, the triple system scenario still needs to solve the following issue: our spectral time series did not reveal any binary motion on a time-scale of a few days. If the primary is indeed constituted of two stars, the short period orbit might be seen under a very low inclination angle. We might also consider the possibility that the time-scale of this orbit is a few weeks or so, and therefore poorly sampled by our spectral time series. However, we note that the radial velocity curve plotted in Fig. 4 does not present any strong dispersion likely to be due to an orbital motion on a time-scale significantly shorter than the main period of 442 d. In addition, we might expect some additional X-rays to be produced by an interaction between the winds of the two stars constituting the primary. High quality data obtained for instance with *XMM-Newton* are strongly needed to investigate the X-ray emission from HD 15558 and discuss its origin in detail. In summary, even though our data do not provide any strong evidence supporting the triple scenario, this scenario may reconcile the mass derived for the primary and its spectral type.

5.3. An open cluster with unusually large stellar masses?

The existence of such a massive star is worth discussing in the context of the massive star population of IC 1805, which should not be addressed without considering the presence of the most evolved object known in the vicinity: the microquasar LSI +61°303. This high mass X-ray binary producing a collimated relativistic jet consists of a Be star and of a compact object whose nature (neutron star or black hole) is not yet established (Massi 2004). LSI +61°303 is believed to have been ejected out of IC 1805 during the supernova explosion of the initially most massive component of the binary (Mirabel et al. 2004). If the progenitor of LSI +61°303 was formed at the same epoch as the other O-stars in IC 1805, among which is HD 15558, its primary component may have been more massive than the primary of HD 15558. Alternatively, if LSI +61°303 was part of an older population of stars, its supernova explosion might have triggered the formation of the current population of O-type stars.

Two additional stars of this cluster are believed to have very large stellar masses, namely HD 15570 and HD 15629 (see Herrero et al. 2000), even though their masses have up to now only been estimated through model atmosphere fits. Unfortunately, as these two stars are probably single, an independant mass determination through the study of a binary motion is unlikely.

Table 3. O-type star content of IC 1805. The first column gives the star number following Vasilevskis et al. (1965). For the multiplicity, "s" means that our investigations did not reveal any indication of binarity, and "?" a lack of spectroscopic monitoring. The references for the spectral types are: (1) Massey et al. (1995); (2) Paper I; (3) Underhill (1967); (4) Ishida (1970); (5) this study.

#	ID	Sp. Type*	Ref.	Status
21		O9.5V((f))	1	?
104	BD +60° 497	O6.5V((f)) + O9V((f))**	2	SB2
112	BD +60° 498	O9V	3	?***
113		O9Ve	4	?
118	BD +60° 499	O9.5V((f))	1	?
138	BD +60° 501	O7V((f))	2	s
148	HD 15558	O5.5III(f) + O7V	5	SB2
160	HD 15570	O4If$^+$	5	s
192	HD 15629	O5((f))	5	s
232	BD +60° 513	O7.5V((f))	2	s

Notes: * the spectral type of the four stars that are not studied in Paper I or in this paper may be uncertain as both O- and B-types were proposed by various authors, ** the spectral type of the secondary should range between O8.5 and O9.5, *** Underhill (1967) reported double lines for this star.

This series of presumably very massive objects suggests that IC 1805 harbours a population of particularly massive stars as compared to other open clusters. According to Massey et al. (1995), a large number of very massive stars in an open cluster may be explained by its youth. Indeed, the age of the massive star population in IC 1805 was estimated to be 2 ± 1 Myr. Its most massive members have therefore not yet evolved into compact objects.

5.4. Multiplicity in IC 1805

The multiplicity of massive stars in young open clusters is a crucial question. The García & Mermilliod (2001) proposal of a binary frequency of 80% for O-stars suggests that the star formation process that was at work in IC 1805 favored the formation of massive binary systems. However, in our spectroscopic study of three mid-O-type stars of this cluster (Rauw & De Becker 2004), we showed that only one system is a spectroscopic binary (BD +60° 497), whilst the other two are most probably single stars (BD +60° 501 and BD +60° 513), leading to the conclusion that the binary frequency claimed by García & Mermilliod (2001) might be overestimated.

In Table 3, we summarize our present knowledge of the multiplicity of the O-star members of IC 1805. At this stage, spectroscopic monitoring confirmed the binarity of only two members, i.e. HD 15558 (this paper) and BD +60° 497 (Paper I; Hillwig et al. 2006), and our investigations revealed no indication of binarity for four of them (BD +60° 501, BD +60° 513, HD 15570 and HD 15629). For the four remaining O-type members, the multiplicity remains an open question. Consequently, at this stage all we can say is that the O-star binary frequency in IC 1805 should be of at least 20% but is most probably not more than 60%.

6. Summary and conclusions

We have presented the results of an intensive spectroscopic study of the brightest massive stars in the young open cluster IC 1805: HD 15570, HD 15629 and HD 15558. For HD 15570

and HD 15629, the RVs do not present any significant trend attributable to binary motion on a time scale of a few days, nor from one year to the next. This is in line with the results obtained by Hillwig et al. (2006) who performed a search for RV variation on time-scales of a few days for some O-type stars of IC 1805 including HD 15629 and HD 15570.

In the case of HD 15558, we have derived an SB1 orbital solution with significantly refined parameters as compared to those obtained by Garmany & Massey (1981). The system appears to be eccentric ($e \sim 0.4$) and we obtain a period of 442 ± 12 d. A careful inspection of the spectra obtained close to the extrema of the radial velocity curve reveals the presence of the companion in the profiles of the He I λ 4471, He II λ 4542, C IV λ 5812 and He I λ 5876 lines. We have simultaneously fitted Gaussians to the profiles of the He I λ 4471 and He II λ 4542 lines in order to separate the primary and secondary components. The determination of the equivalent width of these two lines allowed us to derive O5.5 and O7 spectral types respectively for both stars. Considering in addition that the He II λ 4686 line of the primary has a P-Cygni profile whilst the same line is in absorption in the case of the secondary, along with the fact that we do not clearly observe the N III $\lambda\lambda$ 4634-4641 lines in emission for the secondary, we propose that HD 15558 is an O5.5III(f) + O7V binary.

We estimated the radial velocities of the secondary of HD 15558 following two approaches: (1) a simultaneous fit of line profiles and (2) a disentangling method. Both techniques allowed us to determine minimum masses of the order of 150 ± 50 and $50 \pm 15\, M_{\odot}$ respectively for the primary and the secondary. We also obtained the first SB2 orbital solution for HD 15558. Although we note that the quality of this SB2 solution is rather poor, our data point clearly to a rather high mass ratio (about 3), leading to an extreme minimum mass for the primary. Our results require independent validation using an improved disentangling procedure.

The main problem in considering our results is to reconcile the very extreme mass of the primary with its spectral type. It is indeed unlikely that a very massive main-sequence star could cool down enough during its evolution to become an O5.5 giant. A possible scenario can however be considered where HD 15558 is not a binary but a triple system. The primary may be a yet unrevealed close binary system. In this case, as the mass of the primary is estimated on the basis of the motion of the secondary, the primary object – i.e. the hypothetical close binary – would appear to be a massive object whose mass is the sum of the masses of two stars. Even though our data do not provide any evidence for this scenario, we estimate that at this stage it should not be rejected, and that it could constitute a valuable working hypothesis for future investigations concerning this system.

From our new and previously published results, we briefly address the question of the multiplicity of the early-type stars in IC 1805. The binary frequency among O-stars should be of at least 20%, since out of 10 O-stars only 2 are confirmed binaries, and should not exceed 60%. We therefore conclude that the previously claimed binary frequency of 80% was overestimated.

Acknowledgements. We gratefully acknowledge the anonymous referee for the careful reading, and for comments that significantly helped us to improve the paper. We are indebted to the FNRS (Belgium) for assistance including contract 1.5.051.00 "Crédit aux chercheurs". The travels to OHP were supported by the Ministère de l'Enseignement Supérieur et de la Recherche de la Communauté Française. This research is also supported in part by contract PAI P5/36 (Belgian Federal Science Policy Office) and through the PRODEX XMM/Integral contract. We thank the staff of the Observatoire de Haute Provence (France) and of the San Pedro Martir Observatory (Mexico) for their technical support. Part of our OHP data were obtained in Service Mode. We are grateful to all the observers and technicians who took good care of our observations. The SIMBAD database has been consulted for the bibliography.

References

Appenzeller, I. 1987, in Instabilities in Luminous Early Type Stars, ASSL, 136, 55
Bagnuolo, W. G., Gies, D. R., Riddle, R., & Penny, L. R. 1999, ApJ, 527, 353
Baranne, A., Queloz, D., Mayor, M., et al. 1996, A&AS, 119, 373
Bonanos, A. Z., Stanek, K. Z., Udalski, A., et al. 2004, ApJ, 611, L33
Bonnell, I. A., & Bate, M. R. 2002, MNRAS, 336, 659
Conti, P. S., Leep, E. M., & Lorre, J. J. 1977, ApJ, 214, 759
De Becker, M. 2005, Ph.D. Thesis, University of Liège
De Becker, M., Rauw, G., & Manfroid, J. 2004, A&A, 424, L39
Eggleton, P. P. 1983, ApJ, 268, 368
Feinstein, A., Vazquez, R. A., & Benvenuto, O. G. 1986, A&A, 159, 223
Figer, D. F., Najarro, F., Morris, M., et al. 1998, ApJ, 506, 384
García, B., & Mermilliod, J. C. 2001, A&A, 368, 122
Garmany, C. D., & Massey, P. 1981, PASP, 93, 500
Gillet, D., Burnage, R., Kohler, D., et al. 1994, A&AS, 108, 181
González, J., & Levato, H. 2006, A&A, 448, 283
Gosset, E., Royer, P., Rauw, G., Manfroid, J., & Vreux, J.-M. 2001, MNRAS, 327, 435
Heck, A., Manfroid, J., & Mersch, G. 1985, A&AS, 59, 63
Herrero, A., Puls, J., & Villamariz, M. R. 2000, A&A, 354, 193
Hillwig, T., Gies, D., Bagnuolo, W., et al. 2006, ApJ, 639, 1069
Howarth, I. D., & Prinja, R. K. 1989, ApJS, 69, 527
Humphreys, R. M. 1978, ApJS, 38, 309
Ishida, K. 1970, PASJ, 22, 277
Martins, F., Schaerer, D., & Hillier, D. J. 2005, A&A, 436, 1049
Massey, P., & Hunter, D. A. 1998, ApJ, 493, 180
Massey, P., Johnson, K. E., & Degioia-Eastwood, K. 1995, ApJ, 454, 151
Massi, M. 2004, in European VLBI Network on New Developments in VLBI Science and Technology, 215
Mathys, G. 1988, A&AS, 76, 427
Mathys, G. 1989, A&AS, 81, 237
Mirabel, I. F., Rodrigues, I., & Liu, Q. Z. 2004, A&A, 422, L29
Oey, M. S., & Clarke, C. J. 2005, ApJ, 620, L43
Raboud, D., & Mermilliod, J.-C. 1998, A&A, 333, 897
Rauw, G., & De Becker, M. 2004, A&A, 421, 693 (Paper I)
Rauw, G., De Becker, M., Nazé, Y., et al. 2004, A&A, 420, L9
Sagar, R., Miakutin, V. I., Piskunov, A. E., & Dluzhnevskaia, O. B. 1988, MNRAS, 234, 831
Sana, H., Hensberge, H., Rauw, G., & Gosset, E. 2003, A&A, 405, 1063
Schaerer, D., Meynet, G., Maeder, A., & Schaller, G. 1993, A&AS, 98, 523
Schaller, G., Schaerer, D., Meynet, G., & Maeder, A. 1992, A&AS, 96, 269
Shi, H. M., & Hu, J. Y. 1999, A&AS, 136, 313
Underhill, A. B. 1967, in IAU Symp. 30: Determination of Radial Velocities and their Applications, 167
Vasilevskis, S., Sanders, W. L., & van Altena, W. F. 1965, AJ, 70, 806
Walborn, N. 2001, in Eta Carinae and Other Mysterious Stars: The Hidden Opportunities of Emission Spectroscopy, ASP Conf. Ser., 242, 217
Walborn, N. R. 1972, AJ, 77, 312
Walborn, N. R., & Fitzpatrick, E. L. 1990, PASP, 102, 379
Werner, K., & Rauch, T. 2001, in Eta Carinae and Other Mysterious Stars: The Hidden Opportunities of Emission Spectroscopy, ASP Conf. Ser., 242, 229
Wolfe, R. H., Horak, H. G., & Storer, N. W. 1967, The machine computation of spectroscopic binary elements (Modern astrophysics. A memorial to Otto Struve), 251

Online Material

Table A.1. Observing runs used for the line profile variability study of HD 15570, HD 15629 and HD 15558. The first and second columns give the name of the campaign as used in the text as well as the instrumentation used. The next columns are the number of spectra obtained, the time elapsed between the first and the last spectrum of the run, the natural width of a peak of the power spectrum taken as $1/\Delta T$, and the mean signal-to-noise ratio of each data set.

Obs. run	Telescope	N	ΔT (d)	$\Delta\nu_{\rm nat}$ (d^{-1})	S/N
HD 15570					
Sept. 2000	OHP/1.52 m	7	9.99	0.10	390
Sept. 2001	OHP/1.52 m	5	7.02	0.14	360
Sept. 2002	OHP/1.52 m	10	14.94	0.07	300
Oct. 2003	OHP/1.52 m	7	17.97	0.06	300
Oct. 2004	OHP/1.52 m	7	9.90	0.10	260
Oct. 2004	SPM/2.10 m	4	2.07	0.48	180
HD 15629					
Sept. 2002	OHP/1.52 m	9	12.99	0.08	300
Oct. 2003	OHP/1.52 m	4	17.98	0.06	280
Oct. 2004	OHP/1.52 m	7	9.90	0.10	260
HD 15558					
Sept. 2000	OHP/1.52 m	12	10.97	0.09	530
Sept. 2001	OHP/1.52 m	12	7.02	0.14	440
Sept. 2002	OHP/1.52 m	11	14.92	0.07	430
Oct. 2003	OHP/1.52 m	7	17.95	0.06	360
Oct. 2004	OHP/1.52 m	5	7.00	0.14	450

Appendix A: Observations and data reduction

Spectroscopic observations were collected at the Observatoire de Haute-Provence (OHP, France) during several observing runs from 2000 to 2004 for HD 15570 and HD 15558, and from 2002 to 2004 for HD 15629. All spectra were obtained with the Aurélie spectrograph fed by the 1.52 m telescope (Gillet et al. 1994), using the same setup as described in Paper I. Our collection of spectra is described in Table A.1.

We also obtained several spectra of HD 15570 with the echelle spectrograph mounted on the 2.1 m telescope at the Observatorio Astronómico Nacional of San Pedro Martir (SPM) in Mexico, with exposure times ranging from 10 to 20 minutes. The instrument covers the spectral domain between about 3800 and 6800 Å. The detector was a Site CCD with 1024×1024 pixels of $24\,\mu m^2$. The slit width was set to $200\,\mu$m corresponding to 2 arcsec on the sky. The data were reduced using the echelle package available within the MIDAS software. After adding consecutive spectra of a given night to reach higher signal-to-noise ratios, at the expense of time resolution, we obtained 4 spectra of HD 15570.

We obtained 17 additional spectra of HD 15558 with the Elodie echelle spectrograph (Baranne et al. 1996) fed by the 1.93 m telescope at the Observatoire de Haute Provence between March 2003 and February 2005 to monitor a complete orbital period. The exposure time of each of these spectra was 90 minutes. This spectrograph uses a combination of a prism and a grism as a cross-disperser, with a blaze angle of 76°. The resolving power achieved is about 42 000 between 3906 and 6811 Å in a single exposure, and the detector is a Tk1024 CCD with $24\,\mu m \times 24\,\mu$m pixels. The Elodie data consist of single spectra distributed over 67 orders. Due to pointing constraints specific to the 1.93 m telescope, no echelle spectra were obtained between April 2004 and July 2004. We filled that gap with 6 observations with the Aurélie spectrograph mounted on the 1.52 m telescope.

Table A.2. Description of the data of HD 15558 obtained during the long-term monitoring using the 1.93 and the 1.52 m telescopes. The first column gives the date of the observation. The instrumentation used to obtain the spectrum is provided in the second column. The next columns give the resolving power of the instrumentation used, and the signal-to-noise ratio.

Date	Telescope/Instr.	$\lambda/\Delta\lambda$	S/N
2003/09/04	1.93 m/Elodie	42 000	170
2003/10/04	1.93 m/Elodie	42 000	160
2003/10/21	1.93 m/Elodie	42 000	100
2004/01/07	1.93 m/Elodie	42 000	180
2004/01/15	1.93 m/Elodie	42 000	100
2004/02/14	1.93 m/Elodie	42 000	130
2004/03/11	1.93 m/Elodie	42 000	110
2004/04/04	1.93 m/Elodie	42 000	110
2004/04/10	1.52 m/Aurélie	8000	330
2004/05/06	1.52 m/Aurélie	16 000	160
2004/06/09	1.52 m/Aurélie	16 000	290
2004/06/28	1.52 m/Aurélie	16 000	360
2004/07/15	1.52 m/Aurélie	8000	550
2004/07/26	1.52 m/Aurélie	16 000	360
2004/08/15	1.93 m/Elodie	42 000	100
2004/08/26	1.93 m/Elodie	42 000	120
2004/09/06	1.93 m/Elodie	42 000	140
2004/10/07	1.93 m/Elodie	42 000	130
2004/11/09	1.93 m/Elodie	42 000	60
2004/11/17	1.93 m/Elodie	42 000	140
2004/12/03	1.93 m/Elodie	42 000	140
2005/01/27	1.93 m/Elodie	42 000	100
2005/02/16	1.93 m/Elodie	42 000	70

Two spectra out of the 6 were obtained using the same grating as described in the previous paragraph (between 4455 and 4890 Å). The four remaining spectra were obtained using a 1200 l/mm grating providing a resolving power of about 16 000 in the blue range, with a reciproqual dispersion of 8 Å mm^{-1} (between 4455 and 4680 Å). The exposure time of these 6 Aurélie spectra was 60 min.

For Aurélie data, we adopted the same reduction procedure as in Paper I. Elodie data were reduced using the standard on-line automatic treatment implemented at the OHP. All spectra were normalized using splines calculated on the basis of properly chosen continuum windows.

Appendix B: Radial velocity measurements

The mean RVs of HD 15570 and HD 15629 obtained for the various observing runs are collected in Table B.1. In the case of HD 15558, all the RVs used to obtain the orbital solution are listed in Table B.2. All the RVs considered in this paper were estimated using the rest wavelengths provided by Conti et al. (1977).

Table B.1. Radial velocity of the main He and N lines for both stars measured on OHP spectra (expressed in km s^{-1}). The mean radial velocity along with its 1-σ standard deviations are provided for each observing run. All individual RVs can be found in the WEBDA data base at `http://obswww.unige.ch/webda`.

Data set	HD 15570			
	He I λ 4471	He II λ 4542	N III λ 4634	N III λ 4641
Sep. 2000	–69.1 ± 8.2	–46.7 ± 8.7	–56.1 ± 3.9	–67.0 ± 2.8
Sep. 2001	–65.1 ± 10.6	–51.1 ± 3.2	–58.6 ± 3.5	–70.3 ± 2.0
Sep. 2002	–60.5 ± 13.2	–50.0 ± 5.0	–56.8 ± 4.6	–70.0 ± 3.3
Oct. 2003	–59.3 ± 15.7	–46.2 ± 3.9	–55.6 ± 4.5	–67.6 ± 5.4
Oct. 2004	–72.7 ± 8.3	–47.8 ± 7.0	–58.0 ± 4.7	–70.6 ± 3.7
All	–65.0 ± 12.3	–48.3 ± 5.9	–56.9 ± 4.2	–69.1 ± 3.8
Data set	HD 15629			
	He I λ 4471	He II λ 4542	N III λ 4634	N III λ 4641
Sep. 2000	–	–	–	–
Sep. 2001	–	–	–	–
Sep. 2002	–60.6 ± 3.6	–46.9 ± 4.5	–59.9 ± 8.8	–72.1 ± 6.8
Oct. 2003	–55.3 ± 4.6	–41.0 ± 1.6	–54.6 ± 3.2	–71.6 ± 2.6
Oct. 2004	–58.2 ± 5.9	–50.1 ± 4.6	–63.5 ± 8.3	–74.6 ± 6.5
All	–58.7 ± 4.9	–46.8 ± 5.2	–60.1 ± 8.2	–72.9 ± 6.0

Table B.2. Radial velocities obtained from our time series of HD 15558. The second and third columns give the heliocentric Julian day (–2 450 000) and the orbital phase following the parameters provided in Table 1 (left part). The next columns provide the radial velocities obtained for lines that were selected for the determination of the SB1 orbital solution. The column labelled "Mean" contains the mean of the radial velocities obtained for the He II and the N III lines quoted in the fourth and fifth columns. All RVs are expressed in km s^{-1}. The last column gives the weight (W) attributed to our measurements to calculate the orbital parameters, depending on the spectral resolution of the instrument and the signal-to-noise ratio of the spectra.

#	HJD	ϕ	He II λ 4542	N III $\lambda\lambda$ 4634, 4641	Mean	W
1	1810.640	0.034	–85.9	–96.1	–91.0	0.25
2	1810.658	0.034	–88.0	–117.0	–102.5	0.25
3	1811.619	0.037	–86.7	–109.0	–97.9	0.25
4	1811.665	0.038	–88.8	–101.5	–95.1	0.25
5	1812.660	0.039	–87.5	–112.6	–100.0	0.25
6	1813.651	0.041	–87.8	–118.8	–103.3	0.25
7	1814.643	0.043	–91.6	–118.9	–105.2	0.25
8	1815.645	0.046	–88.9	–110.2	–99.6	0.25
9	1818.641	0.053	–86.4	–110.6	–98.5	0.25
10	1819.593	0.055	–86.8	–109.9	–98.3	0.25
11	1820.648	0.057	–83.0	–118.1	–100.6	0.25
12	1821.609	0.059	–91.2	–111.2	–101.2	0.25
13	2163.580	0.832	–1.2	–12.1	–6.7	0.25
14	2164.597	0.834	–4.3	–10.4	–7.3	0.25
15	2164.660	0.835	–0.9	–18.8	–9.9	0.25
16	2165.577	0.837	–3.5	–23.7	–13.6	0.25
17	2165.590	0.837	–0.1	–12.9	–6.5	0.25
18	2167.550	0.841	–1.9	–7.4	–4.6	0.25
19	2167.564	0.841	–6.7	–14.8	–10.7	0.25
20	2168.601	0.843	–1.8	–17.3	–9.5	0.25
21	2168.642	0.844	–6.0	–18.9	–12.4	0.25
22	2169.581	0.846	–4.2	–16.8	–10.5	0.25
23	2170.580	0.848	–7.2	–22.1	–14.6	0.25
24	2170.603	0.848	–8.1	–23.9	–16.0	0.25
25	2518.617	0.634	–27.5	–28.5	–28.0	0.25
26	2520.593	0.639	–14.8	–20.2	–17.5	0.25
27	2523.580	0.646	–11.5	–32.8	–22.2	0.25
28	2524.510	0.648	–13.8	–28.0	–20.9	0.25
29	2527.531	0.655	–12.4	–21.6	–17.0	0.25
30	2528.499	0.657	–14.5	–26.7	–20.6	0.25
31	2529.529	0.659	–10.5	–21.6	–16.1	0.25
32	2531.503	0.664	–4.9	–21.8	–13.4	0.25
33	2532.516	0.666	–8.3	–20.6	–14.5	0.25
34	2532.644	0.666	–7.9	–27.2	–17.5	0.25
35	2533.532	0.668	–12.6	–24.2	–18.4	0.25
36	2886.627	0.466	–37.0	–51.5	–44.2	1.00
37	2916.592	0.534	–29.4	–62.0	–45.7	1.00
38	2916.558	0.534	–24.7	–39.1	–31.9	0.25
39	2918.570	0.538	–25.7	–52.6	–39.2	0.25
40	2919.561	0.541	–26.6	–47.8	–37.2	0.25
41	2922.566	0.547	–24.4	–34.4	–29.4	0.25
42	2926.573	0.556	–19.6	–34.8	–27.2	0.25
43	2928.593	0.561	–24.7	–39.4	–32.0	0.25
44	2934.511	0.574	–20.0	–33.2	–26.6	0.25

Table B.2. continued.

#	HJD	ϕ	He II λ 4542	N III $\lambda\lambda$ 4634, 4641	Mean	W
45	2934.481	0.574	–13.7	–47.1	–30.4	1.00
46	3012.476	0.751	–14.0	–31.5	–22.7	1.00
47	3020.329	0.768	–19.2	–20.7	–20.0	1.00
48	3050.375	0.836	–11.2	–24.6	–17.9	1.00
49	3076.317	0.895	–16.7	–34.3	–25.5	1.00
50	3100.318	0.949	–43.1	–62.1	–52.6	1.00
51	3106.340	0.963	–28.8	–47.1	–38.0	0.25
52	3132.374	0.022	–63.5	–85.2	–74.3	0.50
53	3165.550	0.097	–88.2	–114.4	–101.3	0.50
54	3184.590	0.140	–82.7	–104.4	–93.6	0.50
55	3201.593	0.178	–72.1	–98.7	–85.4	0.25
56	3212.544	0.203	–65.3	–94.9	–80.1	0.50
57	3232.579	0.248	–67.1	–87.5	–77.3	1.00
58	3244.384	0.275	–63.0	–93.0	–78.0	1.00
59	3254.630	0.298	–46.3	–78.0	–62.2	1.00
60	3286.477	0.370	–43.8	–60.1	–52.0	1.00
61	3289.570	0.377	–46.3	–62.9	–54.6	0.25
62	3290.553	0.379	–35.6	–53.3	–44.4	0.25
63	3294.603	0.388	–32.3	–46.6	–39.4	0.25
64	3295.584	0.390	–37.6	–44.2	–40.9	0.25
65	3296.569	0.393	–44.0	–56.0	–50.0	0.25
66	3318.587	0.442	–28.5	–41.8	–35.1	0.10
67	3326.508	0.460	–33.4	–56.5	–45.0	1.00
68	3343.487	0.499	–27.9	–54.4	–41.2	1.00
69	3398.308	0.623	–9.4	–33.8	–21.6	1.00
70	3418.295	0.668	–3.6	–24.5	–14.0	0.10